FISEVIER

Contents lists available at ScienceDirect

Commun Nonlinear Sci Numer Simulat

journal homepage: www.elsevier.com/locate/cnsns



Dynamical and statistical properties of a rotating oval billiard



Diogo Ricardo da Costa a,b,*, Diego F.M. Oliveira c, Edson D. Leonel c,d

- ^a Instituto de Física, Univ São Paulo, Rua do Matão, Cidade Universitária, 05314-970 São Paulo, SP, Brazil
- ^b School of Mathematics, University of Bristol, Bristol BS8 1TW, United Kingdom
- ^c UNESP, Univ Estadual Paulista, Departamento de Física, Av. 24A 1515, Bela Vista, 13506-900 Rio Claro, SP, Brazil
- ^d The Abdus Salam ICTP, Strada Costiera, 11, 34151 Trieste, Italy

ARTICLE INFO

Article history:
Received 26 March 2013
Received in revised form 6 August 2013
Accepted 6 October 2013
Available online 22 October 2013

Keywords: Rotating oval billiard Dynamical properties Chaos

ABSTRACT

Some dynamical and statistical properties of a time-dependent rotating oval billiard are studied. We considered cases with (i) positive and (ii) negative curvature for the boundary. For (i) we show the system does not present unlimited energy growth. For case (ii) however the average velocity for an ensemble of noninteracting particles grows as a power law with acceleration exponent well defined. Finally, we show for both cases that after introducing time-dependent perturbation, the mixed structure of the phase space observed for static case is recovered by making a suitable transformation in the angular position of the particle.

© 2013 Elsevier B.V. All rights reserved.

1. Introduction

As an attempt to explain the origin of cosmic rays acceleration, Enrico Fermi [1], in his pioneering work, proposed that charged particles could be accelerated by collisions/interactions with time-dependent magnetic structures. Since then, many models have been proposed in order to understand/explain Fermi's idea [2–13] (and references in therein).

One of the most studied version of the problem is the one-dimensional Fermi–Ulam model [14–17]. Such a system consists of a classical particle (representing the cosmic particle) confined and bouncing between two rigid walls, one of them is assumed to be fixed (working as a returning mechanism) and the other one moves periodically in time (denoting the time-dependent magnetic structure). It has been proved [18] that in such a system the unlimited energy growth, also known as Fermi acceleration, is not observed due to the existence of a set of invariant spanning curves in the phase space, therefore the model fails to produce unlimited energy growth. On the other hand, if the fixed wall is replaced by a constant gravitational field, for a specific combination of initial conditions and control parameters the unlimited energy growth can be observed [19,20]. This happens due to the loss of correlation between two collisions since as the velocity increases, the time between collisions also increases.

A natural extension of one-dimension systems are two-dimensional billiards model. In such systems one or many (non-interacting) particles are confined in a closed domain experiencing collisions with the boundary [21–24]. Basically they can be classified in three different classes namely, (i) integrable, (ii) ergodic and (iii) mixed. One of the main questions about such systems is whether or not the unlimited energy growth of the particle is observed. In this sense, a conjecture by Loskutov–Ryabov–Akinshin (LRA) has been proposed [25]. Basically the conjecture states that, if the system has a chaotic component in the phase space for the static version of the problem, after the introduction of a time-dependent perturbation on the boundary, the phenomenon of Fermi acceleration must be observed. Such a conjecture has been confirmed in many billiards including, oval [26,27], stadium [28], Lorentz gas [29–31] and many others. Recently it has been shown that even elliptic

^{*} Corresponding author at: Instituto de Física, Univ São Paulo, Rua do Matão, Cidade Universitária, 05314-970 São Paulo, SP, Brazil. Tel.: +55 1982781422. E-mail address: drcosta@usp.br (D.R. da Costa).

billiards [32–34], whose integrability comes from the conservation of the angular momenta with respect to the two foci [35], after the introduction of a time-dependent perturbation on the boundary, the unlimited energy growth is observed. Such a surprising result happens because the time-dependent perturbation destroys the separatrix given place to a chaotic layer. Thus, those trajectories that used to be confined inside the separatrix can move outside (and the other way around) and this changing of behaviour makes the energy increase.

In this work we consider the dynamics of a classical particle experiencing elastic collisions with a time-dependent rotating oval billiard. We are seeking to understand and describe the behaviour of the average velocity for an ensemble of non interacting particles in two regimes of the boundary: (i) positive curvature; (ii) locally negative curvature. The structure of the phase space depends on the control parameters and we show that even after the introduction of a time-dependent perturbation the structure of the phase space observed for the static case can be recovered by making a suitable transformation on the angular position of the particle. We also study some statistical properties mainly regarding the behaviour of the average velocity for an ensemble of initial conditions. We show that unlimited energy growth is not observed when the shape of the boundary is strictly positive. On the other hand, if regions of nonpositive curvature appears on the boundary, the unlimited energy growth is observed as predicted by LRA-conjecture.

The paper is organized as follows. In Section 2, we present all the details needed to construct the mapping that describes the dynamics of the model. The numerical results are shown in Section 3. Finally, we present our concluding remarks in Section 4.

2. The model and the map

In this section we present all the necessary details to construct the mapping that describes the dynamics of the system. The model consists of a classical particle confined and experiencing collisions with a time-dependent oval billiard. The dynamics of the particle is described in terms of a four-dimensional nonlinear mapping $T(\theta_n, \alpha_n, |\vec{V}_n|, t_n) = (\theta_{n+1}, \alpha_{n+1}, |\vec{V}_{n+1}|, t_{n+1})$ where the variables are: (θ) the angular position of the particle; (α) the angle that the trajectory of the particle forms with the tangent line at the position of the collision; $(|\vec{V}_{n+1}|)$ the absolute velocity of the particle and; (t) the instant of the collision with the boundary. The shape of the boundary in polar coordinates is given by

$$R_b(\theta, p, \epsilon, t) = 1 + \epsilon \cos[p\theta'(t)],\tag{1}$$

where $\epsilon \in [0,1)$ is the parameter which controls the deformation of the boundary, p is a positive integer number, $\theta'(t) = \theta + \omega t$, where ω defines the frequency of rotation and t is the instant of collision. It is important to emphasise that by making such a transformation in θ the time-dependent perturbation acts on the radius of the billiard producing a rotation. If $\omega = 0$, we have the static boundary case [36]. For $\omega \neq 0$ the boundary rotates with angular velocity ω . Additionally, the Cartesian components of the boundary at position (θ_n, t_n) are given by

$$X(\theta_n, t_n) = [1 + \epsilon \cos[p\theta'(t)]] \cos(\theta_n), \tag{2}$$

$$Y(\theta_n, t_n) = [1 + \epsilon \cos[p\theta'(t)]] \sin(\theta_n). \tag{3}$$

Starting with initial condition $(\theta_n, \alpha_n, |V_n|, t_n)$, the angle between the tangent at the boundary and the horizontal axis at the point $X(\theta_n)$ and $Y(\theta_n)$ is given by $\phi_n = \arctan[Y'(\theta_n)/X'(\theta_n)]$, where $X' = dX/d\theta$ and $Y' = dY/d\theta$. Since there are no forces acting on the particle during the flight, its trajectory is a straight line. For $t > t_n$ the position of the particle as a function of time is given by

$$X_p(t) = X(\theta_n, t_n) + |\overrightarrow{V}_n| \cos(\alpha_n + \phi_n)(t - t_n), \tag{4}$$

$$Y_{p}(t) = Y(\theta_{n}, t_{n}) + |\vec{V}_{n}| \sin(\alpha_{n} + \phi_{n})(t - t_{n}). \tag{5}$$

Once the position of the particle as a function of the time is known, its distance measured with respect to the origin of the coordinate system is given by $R_p(\theta_p,t_n)=\sqrt{X_p^2(t)+Y_p^2(t)}$ and θ_p at $X_p(t),Y_p(t)$ is $\theta_p=\arctan[Y_p(t)/X_p(t)]$. The angular position at the next collision of the particle with the boundary, i.e. θ_{n+1} , is numerically obtained by solving the following equation $R_p(\theta,t)=R_b(\theta,t)$ which means that the position of the particle is the same as the boundary, therefore, a collision. The time is obtained by

$$t_{n+1} = t_n + \frac{\sqrt{\Delta X^2 + \Delta Y^2}}{|\vec{V}_n|},$$
 (6)

where $\Delta X = X(\theta_{n+1}) - X(\theta_n)$ and $\Delta Y = Y(\theta_{n+1}) - Y(\theta_n)$. To obtain the new velocity we should note that the referential frame of the boundary is moving. Thus, according to our construction, at the instant of collision, the following conditions must be matched

$$\vec{V}'_{n+1} \cdot \vec{T}_{n+1} = \vec{V}'_n \cdot \vec{T}_{n+1},\tag{7}$$

$$\vec{V}'_{n+1} \cdot \vec{N}_{n+1} = -\vec{V}'_n \cdot \vec{N}_{n+1},\tag{8}$$

where \vec{T} and \vec{N} are the unit tangent and normal vectors and \vec{V}' denotes the velocity of the particle measured in the moving referential frame. Based on these two last equations, the particle's velocity components after collisions are given by

$$\vec{V}_{n+1} \cdot \vec{T}_{n+1} = |\vec{V}_n|[\cos(\alpha_n + \phi_n)\cos(\phi_{n+1})] + |\vec{V}_n|[\sin(\alpha_n + \phi_n)\sin(\phi_{n+1})], \tag{9}$$

$$\vec{V}_{n+1} \cdot \vec{N}_{n+1} = -|\vec{V}_n|[\sin(\alpha_n + \phi_n)\cos(\phi_{n+1})] + |\vec{V}_n|[\cos(\alpha_n + \phi_n)\sin(\phi_{n+1})] + 2\vec{V}_b(t_{n+1}) \cdot \vec{N}_{n+1}, \tag{10}$$

where $\vec{V}_b(t_{n+1})$ is the velocity of the boundary and $\vec{V}_b(t_{n+1}) \cdot \vec{N}_{n+1}$ is written as

$$\vec{V}_b(t_{n+1}) \cdot \vec{N}_{n+1} = -\epsilon p\omega \sin[p\theta'(t_{n+1})] \times [-\cos(\theta_{n+1})\sin(\phi_{n+1}) + \sin(\theta_{n+1})\cos(\phi_{n+1})]. \tag{11}$$

Therefore, the velocity of the particle at collision (n + 1) is given by

$$|\vec{V}_{n+1}| = \sqrt{(\vec{V}_{n+1} \cdot \vec{T}_{n+1})^2 + (\vec{V}_{n+1} \cdot \vec{N}_{n+1})^2}.$$
 (12)

Finally, α_{n+1} is obtained by

$$\alpha_{n+1} = \arctan\left[\frac{\vec{V}_{n+1} \cdot \vec{N}_{n+1}}{\vec{V}_{n+1} \cdot \vec{T}_{n+1}}\right]. \tag{13}$$

3. Numerical results

In this section we present our numerical results. It is known that for a fixed value of p and ϵ , there is a critical parameter where the curvature of the boundary changes from positive to neutral and then is locally negative [36]. Such a criteria is given by

$$\epsilon_c = \frac{1}{1+p^2}, \quad p \geqslant 1. \tag{14}$$

If $\epsilon < \epsilon_c$ (see Fig. 1(a) for an example of boundary with $\epsilon = 0.1$ and p = 2), the phase space for the time-independent case is mixed with a chaotic sea, Kolmogorov–Arnold–Moser islands and a set of invariant spanning curves. On the other hand, as ϵ increases and becomes larger than ϵ_c the boundary changes and some regions of negative curvature appear (see Fig. 1(b) for an example of boundary with $\epsilon = 0.3$ and p = 2). As a consequence, the invariant tori, corresponding to the whispering gallery orbits are destroyed. For all simulations we considered p = 2 leading to $\epsilon_c = 0.2$. Our results are divided in two cases, namely (i) $\epsilon < \epsilon_c$ and (ii) $\epsilon > \epsilon_c$. As we shall show, for case (i), the phenomenon of Fermi acceleration was not observed, at least for the combination of control parameters and initial conditions considered in the present work. On the other hand, we show that the unlimited energy growth is observed for case (ii) as predicted by LRA-conjecture.

3.1. Case (i): $\epsilon < \epsilon_c$

Fig. 2 shows the behavior of a single initial condition evolved up to $n=2\times 10^5$ collisions with the boundary for the oval billiard. The initial condition used was $\theta_0=\pi,\alpha_0=\pi/2-0.1,V_0=3$, $t_0=0$ and in (a) $\omega=0$ where a large chaotic sea and a period two elliptic fixed point represented by red bullets can be seen. Fig. 2(b) shows the orbit for the rotating billiard considering $\omega=1$. As one can see the structure shown in Fig. 2(a) is not observed. However, applying the transformation $\theta'\to\theta+\omega t$ a similar structure observed in Fig. 2(a) is obtained as can be seen in Fig. 2(c). The position and shape of the KAM islands change and depend on the initial velocity since for an initial velocity larger than the velocity of the boundary,

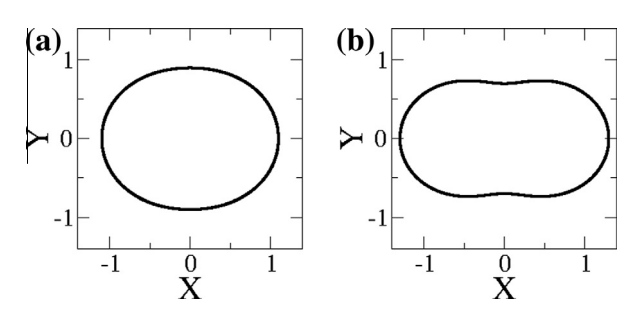


Fig. 1. Boundaries for $p = 2, \omega = 0$ and considering: (a) $\epsilon = 0.1$ and (b) $\epsilon = 0.3$. These are two examples of positive and locally negative curvatures, repectively.

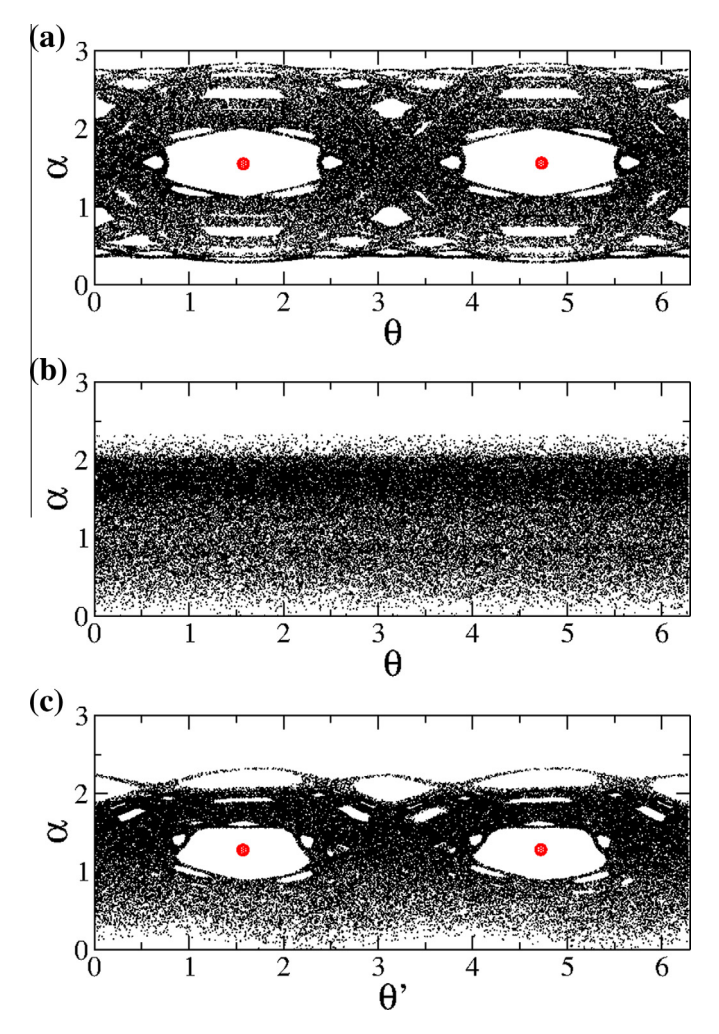


Fig. 2. Plot of: (a) $\alpha \times \theta$ for $\omega = 0$; (b) $\alpha \times \theta$ for $\omega = 1$ and; (c) $\alpha \times \theta'$, where $\theta' = (\theta + \omega t) \pmod{2\pi}$. The parameter used was $\epsilon = 0.1$ and the initial condition was $V_0 = 3$, $\theta_0 = \pi$, $t_0 = 0$ and $\alpha_0 = \pi/2 - 0.1$. The orbit was evolved up to 2×10^5 collisions with the boundary.

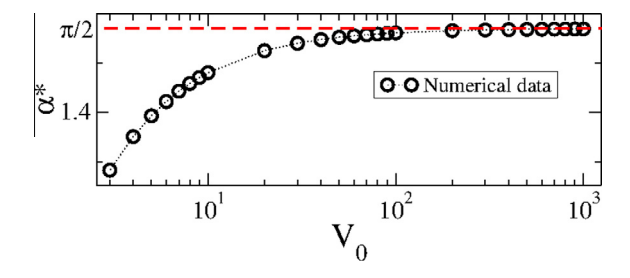


Fig. 3. Plot of the angular coordinate for the period two elliptic fixed point for different values of V_0 and using $\epsilon = 0.1$ and $\omega = 1$. The dashed line is given by $\alpha^* = \pi/2$.

the particle experiences many collisions in a small interval of time and, in the limit of $V \to \infty$ the phase space for the static case is expected to be obtained. Additionally we obtained the angle α^* for the period two elliptic fixed point represented by red¹ bullets in the Fig. 2(c) as a function of V_0 as shown in Fig. 3. Observe that in the limit of $V_0 \to \infty$ leads to $\alpha \to \pi/2$. Fig. 4 shows the behavior of $V \times \theta'$ for $\epsilon = 0.1$, $\alpha_0 = \pi/2 - 0.1$ and $\theta_0 = 0.16$ and considering different values of the initial velocity V_0 evolved up to 10^4 times. Note that for different values of V_0 , the structures observed for the plane $V \times \theta'$ are quite similar (see

¹ For interpretation of color in Fig. 2, the reader is referred to the web version of this article.

Fig. 4). The evolution of the dynamics leads the velocity of the particle to change within a certain range producing separated structures which are not connected to each other. We have performed and extensive numerical simulation by changing the initial conditions, namely α , θ and t for fixed values of V_0 as well as the number of collisions n and we have observed that the velocity is always confined inside the regions shown in Fig. 4. Additionally, the evolution of the average velocity (\overline{V}) as a function of the number of collisions shows that $\overline{V} \to cte$ as $n \to \infty$. Therefore considering the set of simulations made we can conclude the the unlimited energy growth is not observed for the case of $\epsilon < \epsilon_c$, namely, the case where the curvature of the boundary is strictly positive.

Fig. 5(a) shows a trajectory for $V_0=3$, $\alpha_0=\pi/2$, $\theta_0=\pi/2$ and $\omega=0$. For such a case the particle just bounces in a diametrical region of the billiard. Considering the case of $\omega=1$ and $V_0=3$, in order to hit the same position on the boundary, α_0 must be changed, because the geometry is rotating [see Fig. 5(b)] however, considering the same transformation made before for θ , namely $\theta'\to\theta+\omega t$, it can be interpreted as if the boundary stays at the same position and the particle moves as an arc-shaped trajectory as shown in Fig. 5(c). Such trajectories are called Larmor circles [37,38]. For a classical particle with mass m and charge q moving with constant velocity v in a plane region with perfectly reflecting convex boundary, if an uniform constant magnetic field B is directed perpendicularly to the plane of motion, the trajectories consist of a series of arcs of circles with the Larmor radius which is defined as

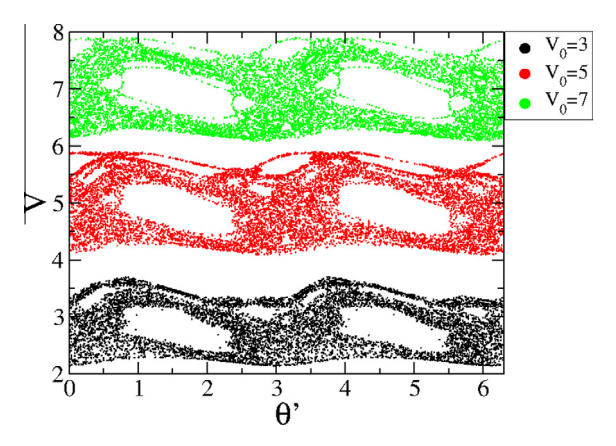


Fig. 4. Plot of V vs. θ' for different values of V_0 and considering $\epsilon = 0.1, \omega = 1, \alpha_0 = \pi/2 - 0.1$ and $\theta_0 = 0.16$. Each orbit was iterated 10^4 times (collisions with the boundary).

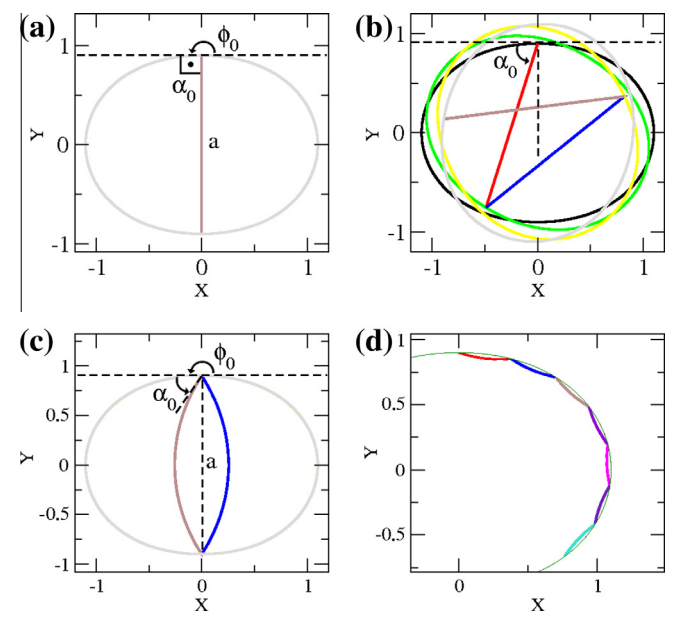


Fig. 5. Plot of an orbit using $V_0 = 3$, $\theta_0 = \pi/2$ and $t_0 = 0$ for: (a) $\omega = 0$ and $\alpha_0 = \pi/2$ (period two elliptic fixed point). This orbit is also called diametral closed orbit [37]; (b) $\omega = 1$ and $\alpha_0 = 1.28312$ (other example of trajectory in a fixed point); (c) Same example shown in item (b) considering the rescale $\theta \to \theta + \omega t$; (d) An example of short skips along the boundary for $\omega = 1$ and $\alpha_0 = 2.9$ (corresponding to a rotator orbit).

$$R_I = m\nu/(aB). \tag{15}$$

where R is proportional to the velocity v and inversely proportional to the magnetic field B. Fig. 5(c) shows an example of such a diametrical and closed orbit. Following [37], we can conclude that $R_L = a/[2\cos(\alpha^*)]$, where a is the distance between the two points of collisions with the boundary. For $\epsilon = 0.1$ and after extensive simulations we obtained $a \cong 1.8$. Fig. 6(a) shows the behavior of R_L as a function of V_0 , and after a power law fit we obtain a slope equal to $0.996(1) \cong 1$, therefore one can conclude that $R_L \propto V_0$. On the other hand, by changing $\omega \in [10^{-3}, 1]$ and R_L , we obtained that $R_L \propto \omega^{-1}$ as shown in Fig. 6(b). Fig. 5(d) shows a rotator orbit, which is an adiabatic regime of short skips along the boundary [37].

Therefore, after some analytical work, for some special situations, it is possible to make a connection between our systems and results obtained for magnetic billiards. It is possible to find analytical expressions for Larmor circles in diametral closed orbits and adiabatic skippings, as shown in Ref. [37]. Other analytical interpretations for this billiard are not so easy to be found, because after the introduction of the time-dependent perturbation we have a 2-dimensional system described by a 4-dimensional map making the calculations harder than the time-independent dynamics.

In order to verify the influence of the corresponding minimum and maximum values of the velocity along the orbit as a function of the initial condition, Fig. 7 shows a plot of the initial conditions $\alpha \times \theta$ where the color denote the extremes of the range of V. For Fig. 7(a) and (c) the color denotes the minimum velocity along the series ranging from 3 to at most 5.5 for the initial velocity of $V_0 = 5$ while Fig. 7(b) and (d) corresponds to the maximum of the velocity along the orbit whose ranges are around 17.5 to 22.5 for $V_0 = 20$. Each orbit was evolved in time until a limit of $n = 10^6$ collisions with the boundary.

3.2. Case (ii): $\epsilon > \epsilon_c$

In this section we consider the case of $\epsilon=0.3>\epsilon_c$. For such a value of ϵ there are two regions with non-positive curvature, one of them near $\pi/2$ and the other one around $3\pi/2$ for the static case. Fig. 8(a) shows an orbit for the time-independent case where $\omega=0$ and considering the initial condition $\alpha_0=\pi/2-0.1$, $\theta_0=\pi$, $t_0=0$ and $V_0=3$. For such a case, one can see the corresponding regions of the KAM islands surrounded by a chaotic sea, however, the set of invariant spanning curves generated from orbits near the border were destroyed. Fig. 8(b) also shows an orbit for the same initial condition of (a) and considering $\omega=1$, after considering the transformation $\theta'=\theta+\omega t$ one can see basically similar structures as observed for the time-independent case.

As part of the numerical investigation for the time-dependent billiard, we studied the behavior of the average velocity as a function of the number of collisions with the boundary for an ensemble non-interacting particles. In our simulations we fixed the initial velocity while the other variables namely, $\theta_0 \in (0, 2\pi]$, $\alpha_0 \in (0, \pi]$ and $t_0 \in (0, 2\pi]$ are taken at random. First, we evaluate the average velocity over the orbit for a single initial condition which is defined as

$$V_i = \frac{1}{n+1} \sum_{i=0}^{n} V_{i,i},\tag{16}$$

where the index *i* corresponds to a sample of an ensemble of initial conditions and the average velocity over an ensemble of initial conditions is written as

$$\overline{V} = \frac{1}{M} \sum_{i=1}^{M} V_i, \tag{17}$$

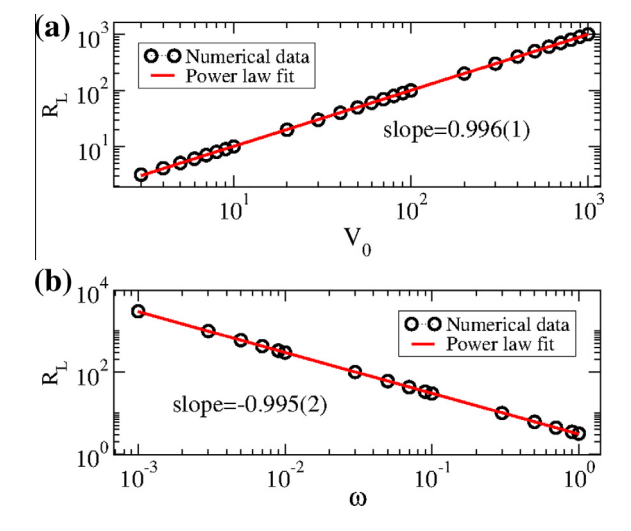


Fig. 6. (a) Plot of R_L as a function of V_0 . After a power law fitting the slope obtained was 0.996(1); (b) $R_L vs. \omega$ and the slope obtained is -0.995(2).

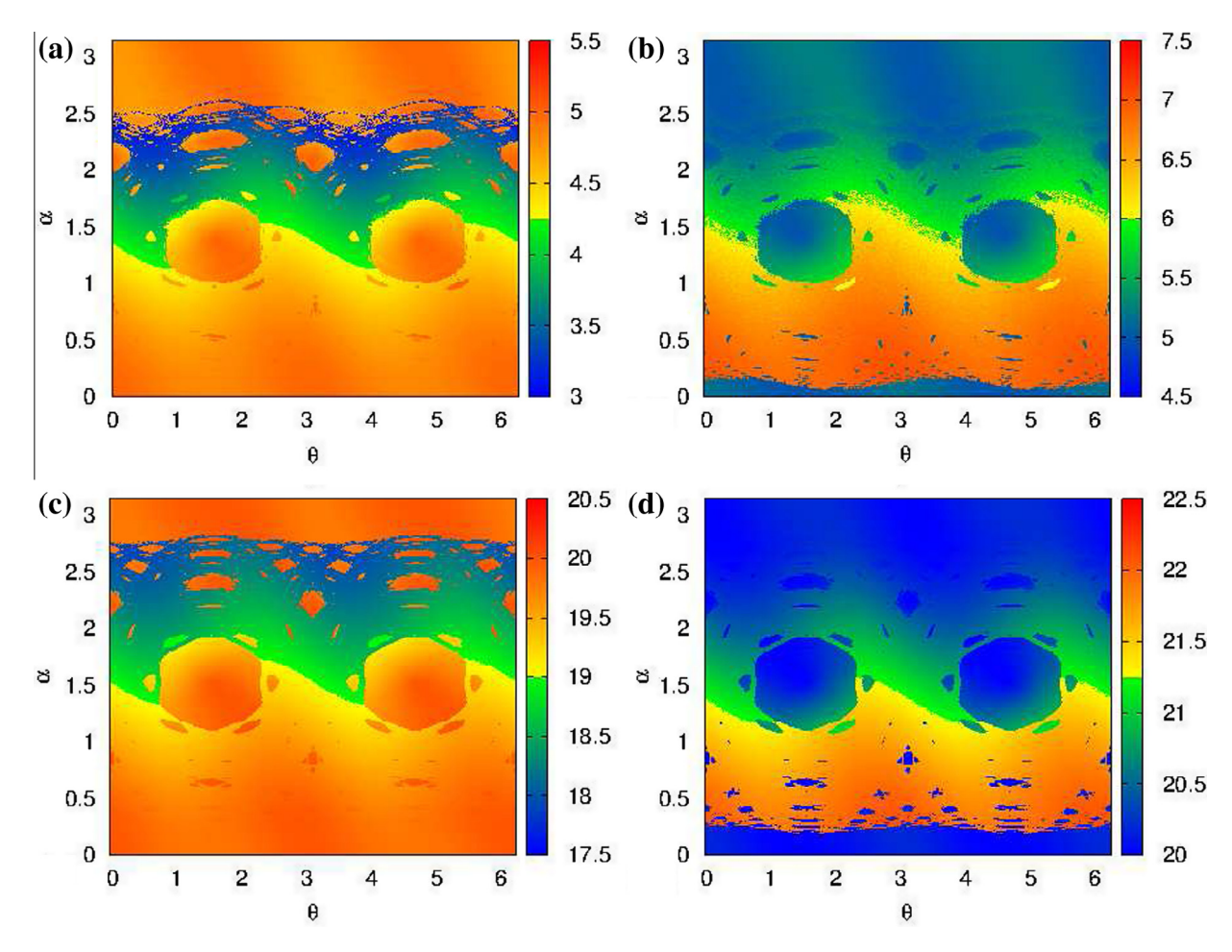
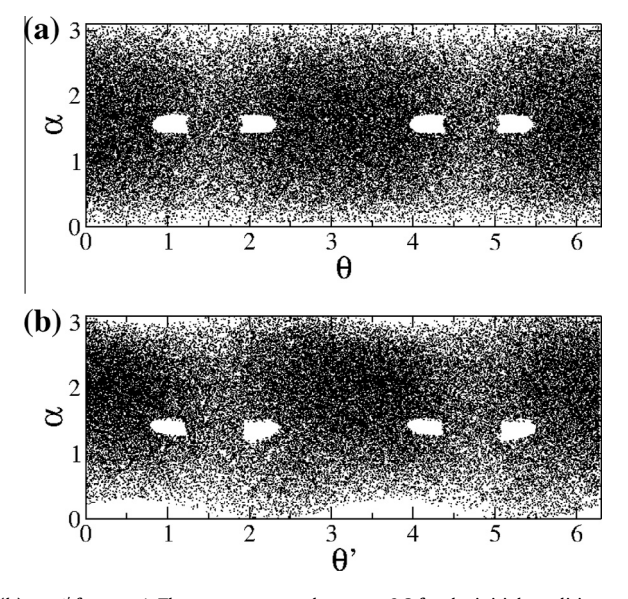


Fig. 7. Diagram of $\alpha \times \theta$ where the color denotes minimum (a,c) and maximum (b,d) velocities along the orbits. The initial time was set as $t_0 = 0$ and: (a,b) $V_0 = 5$ and (c,d) $V_0 = 20$.



 $\textbf{Fig. 8.} \ \ \text{Plot of: (a)} \ \alpha \times \theta \ \text{for } \omega = 0 \ \text{and; (b)} \ \alpha \times \theta' \ \text{for } \omega = 1. \ \text{The parameter used was} \ \epsilon = 0.3 \ \text{for the initial condition} \ \alpha_0 = \pi/2 - 0.1, \ \theta_0 = \pi, t_0 = 0 \ \text{and} \ V_0 = 3.$

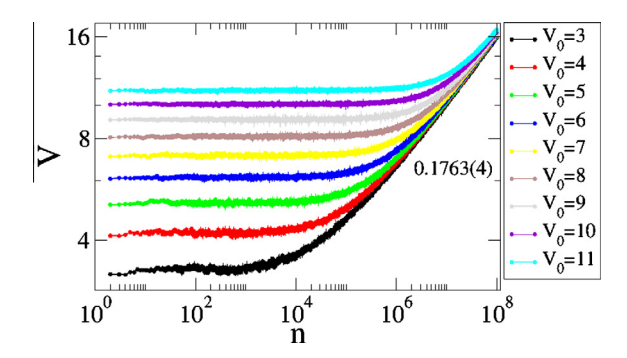


Fig. 9. Behaviour of \overline{V} as a function of n for an ensemble of 300 different initial conditions chosen randomly ($t_0 \in (0, 2\pi], \theta_0 \in (0, 2\pi]$ and $\alpha_0 \in (0, \pi]$) for each V_0 . All orbits were iterated up to 10^8 .

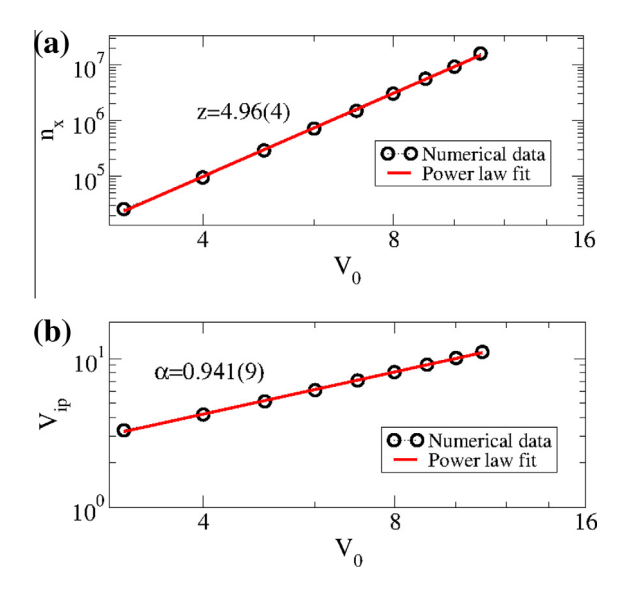


Fig. 10. (a) Plot of $n_x vs. V_0$. A power law fitting gives a slope of z = 4.96(4); (b) Plot of the velocity of the initial plateau V_{ip} as function of V_0 . A power law fitting furnishes $\alpha = 0.941(9)$.

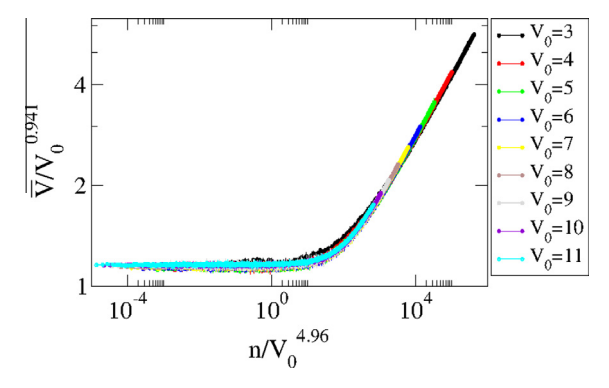


Fig. 11. Rescale of all curves shown in Fig. 9 to a single and universal plot. The transformations used were $(V \to V/V_0^{0.941})$ and $(n \to n/V_0^{4.96})$.

where M = 300 denotes the number of different initial conditions. Fig. 9 shows the behavior of the average velocity as a function of n for nine different initial velocities, as labeled in the figure. As one can see, for short time all the curves remain constant, and after a crossover, $n_{\rm s}^2 = n_{\rm s}$, all of them start to grow together with the same acceleration exponent, namely $\beta = 0.1763(4) \approx 1/6$. It is important to mention that such an acceleration exponent is the same as the one obtained for the

² The crossover number is defined as the intersection between the line of the initial plateau and the acceleration line.

conformally breathing fully chaotic billiards [26,39]. As the initial velocity increases, the crossover number also changes. Fig. 10(a) shows the behaviour of n_x as function of V_0 and after a power law fitting we obtained the exponent z=4.96(4). On the other hand, considering the behavior of the velocity of the initial plateau as a function of the initial velocity, after a power law fitting, we obtained the exponent $\alpha=0.941(9)$. Using these results we can rescale the curves shown in Fig. 9 by making the transformations $V \to V/V_0^{0.941}$ and $n \to n/V_0^{4.96}$ leading all curves to collapse onto a single and universal plot as shown in Fig. 11. Such a result allow us to conclude that the system is scaling invariant and the unlimited energy growth is observed, confirming, therefore, the LRA-conjecture for the case $\epsilon > \epsilon_c$.

4. Conclusions

We have studied some dynamical properties of a time-dependent rotating oval billiard. We have obtained a four dimensional nonlinear map that describes the dynamics of the system. For the case where the curvature of boundary is strictly positive, namely $\epsilon < \epsilon_c$, we have shown that the velocity is always confined to a certain range which depends on the initial velocity and such a behaviour prevents the unlimited energy growth, at least for the control parameters considered. Additionally, we have shown that the angular position can be rescaled such as the trajectories of the particle move through Larmor circles making then a connection between the magnetic billiard and rotating billiard possible. For the case where the boundary has non-positive curvature ($\epsilon > \epsilon_c$), we have shown that the unlimited energy growth is observed confirming the LRA-conjecture and the average velocity is scaling invariant with respect to the initial velocity as well as the number of collisions with the boundary.

Acknowledgments

DRC acknowledges Brazilian agency FAPESP (2012/18962-0 and 2010/52709-5). DFMO is very grateful for the hospitality of Prof. Leonel in his group and for the several discussions we have had along this wonderful and productive time. He is also grateful to FAPESP (2013/01449-1) for supporting his visit to Rio Claro – Brazil during two months – March and April 2013. EDL acknowledges the financial support by FAPESP (2012/23688-5), CNPq and FUNDUNESP, Brazilian agencies. This research was supported in part by FINEP and FAPESP through the computational resources provided by the Center for Scientific Computing (NCC/GridUNESP) of the São Paulo State University (UNESP).

References

[39] Batistić B, Robnik M. J Phys A: Math Theor 2011;44:365101.

```
[1] Fermi E. Phys Rev 1949;75:1169-74.
 [2] Sklarz SE, Tannor DJ, Khaneja N. Phys Rev A 2004;69:053408.
 [3] Gommers R, Bergamini S, Renzoni F. Phys Rev Lett 2005;95:073003.
 [4] Steiner M, Freitag M, Perebeinos V, Tsang JC, Small JP, Kinoshita M, Yuan D, Liu J, Avouris P. Nat Nanotechnol 2009;4:320.
 [5] Nakamura K, Harayama T. Quantum Chaos and Quantum Dots. Oxford: Oxford University Press; 2004.
 [6] Ulam S. Proc. 4th Berkeley Symposium on Math, Statistics and Probability, vol. 3. Berkeley, CA: California University Press; 1961. p. 315.
 [7] Lichtenberg AJ, Lieberman MA. Regular and Chaotic Dynamics. Appl. Math. Sci., vol. 38. New York: Springer Verlag; 1992.
 [8] Everson RM. Physica D 1986;19:355.
 [9] Dembinski ST, Makowski AJ, Peplowski P. Phys Rev Lett 1993;70:1093.
[10] Lichtenberg AJ, Lieberman MA, Cohen RH. Physica D 1980;1:291.
[11] Holmes PJ. J Sound Vibr 1982;84:173.
[12] Tsang KY, Lieberman MA. Physica D 1984;11:147.
[13] Lieberman MA, Tsang KY. Phys Rev Lett 1985;55:908.
[14] José JV, Cordery R. Phys Rev Lett 1986;56:290.
[15] Leonel ED, McClintock PVE, Silva JKL. Phys Rev Lett 2004;93:014101.
[16] Ladeira DG, da Silva JKL. Phys Rev E 2006;73:026201.
[17] Karlis AK, Papachristou PK, Diakonos FK, Constantoudis V, Schmelcher P. Phys Rev Lett 2006;97:194102.
[18] Douady R, Application du theoreme des tores invariants. These de 3eme Cycle. University of Paris VII, 1982.
[19] Pustyl'nikov LD. Russ Math Surv 1995;50:145.
[20] Pustyl'nikov LD. Theoret Math Phys 1988;77:1110.
[21] Dettmann CP, Georgiou O. Phys Rev E 2011;83:036212.
[22] Courbage M, Edelman M, Saberi Fathi SM, Zaslavsky GM. Phys Rev E 2008;77:036203.
[23] Leonel ED, Bunimovich LA. Phys Rev E 2010;82:016202.
[24] Andreasen J, Cao H, Wiersig J, Motter AE. Phys Rev Lett 2009;103:154101.
[25] Loskutov A, Ryabov AB, Akinshin LG. J Phys A 2000;33:7973.
[26] Leonel ED, Oliveira DFM, Loskutov A. Chaos 2009;19:033142.
[27] Oliveira DFM, Leonel ED. Physica A 2010;389:1009.
[28] Loskutov A, Ryabov A. J Stat Phys 2002;108:995.
[29] Oliveira DFM, Leonel ED. Chaos 2012;22:026123.
[30] Oliveira DFM, Vollmer J, Leonel ED. Physica D 2011;240:389.
[31] Karlis AK, Papachristou PK, Diakonos FK, Constantoudis V, Schmelcher P. Phys Rev E 2007;76:016214.
[32] Lenz F, Diakonos FK, Schmelcher P. Phys Rev Lett 2008;100:203.
[33] Leonel ED, Bunimovich LA. Phys Rev Lett 2010;104:224101.
[34] Oliveira DFM, Robnik M. Phys Rev E 2011;83:026202.
[35] Berry MV. Eur J Phys 1981;2:91.
[36] Oliveira DFM, Leonel ED. Commun Nonlinear Sci Numer Simul 2010;15:1092.
[37] Robnik M, Berry MV. J Phys A: Math Gen 1985;18:1361-78.
[38] Berry MV, Sinclair EC. J Phys A: Math Gen 1997;30:2853-61.
```